

Lifetimes and Branching Ratios in Ca^{42} Employing the $(p, p'\gamma)$ Reaction*

W. J. KOSSLER AND J. WINKLER

Massachusetts Institute of Technology, Cambridge, Massachusetts 02139

AND

C. D. KAVALOSKI†

Lowell Technological Institute, Lowell, Massachusetts

(Received 19 August 1968)

The $(p, p'\gamma)$ reaction has been used to study Ca^{42} . Back-scattered protons were detected in an annular solid-state detector of 0.8-sr solid angle. The γ rays were detected in a 32-cc Ge(Li) detector placed at 55° and 125° with respect to the beam. By the Doppler-shift attenuation method (DSAM) the lifetimes of states in Ca^{42} with the following energies have been measured: 2.422 MeV [0.30(+0.04, -0.03) psec]; 2.750 MeV [3.4(+11, -0.17) psec]; 3.250 MeV [0.3(+0.15, -0.10) psec]; 3.297 MeV [3.4(+∞, -2.1) psec]; 3.389 MeV (0.325±0.075 psec); 3.442 MeV [1.35(+1.3, -1) psec]; and 3.651 MeV [0.06(±0.08, -0.06) psec]. The 1.523-MeV 2^+ state was measured to have a lifetime in close agreement with the known lifetimes. The Doppler shift on the 4.43-MeV state in C^{12} was also measured. Branching ratios are reported for 14 states. The reduced matrix elements $B(\sigma\lambda)$ are given for 26 transitions. On the basis of branching-ratio information, $B(\sigma\lambda)$, and previously existing information, spin and parity inferences have been made for the following states: 3.250 MeV (4^+); 3.297 MeV ($2^+, 1^-$); 3.883 MeV ($1^-, 2^+$); and 4.043 MeV ($2^+, 3^-, 4^+$). For other states, we support recent assignments from (t, p) data. Our transition rates for the 2.422-MeV (2^+), 2.750-MeV (4^+), and 3.250-MeV (4^+) states show strong enhancement over single-particle rates. These results, together with the known enhanced rates for the 1.523-MeV (2^+) and 1.836-MeV (0^+) states, strongly support the interpretation of the low-lying levels in Ca^{42} as mixtures of a rotational band and simple shell-model configurations. The level at 3.250 MeV, (4^+) fits naturally into this scheme.

I. INTRODUCTION

NUCLEI in the $f_{7/2}$ shell have been the subject of intensive experimental investigation,¹⁻¹⁹ primarily because of the opportunity they present for comparison with shell-model calculations employing relatively

simple configurations.²⁰⁻²³ The calcium isotopes are particularly interesting in this regard since, in a simple description, the low-lying levels are accounted for by couplings of the $f_{7/2}$ neutrons only. Thus, for example, one would expect a sequence of excited states of Ca^{42} with $J^\pi=0^+, 2^+, 4^+$, and 6^+ . Furthermore, the nucleus Ti^{50} , with two $f_{7/2}$ protons outside the doubly magic Ca^{48} core, should exhibit the same spectrum. Under the assumption of charge independence of the nuclear force, corresponding levels in the two nuclei should be at the same excitation energy. Experimentally, one does observe such a $0^+, 2^+, 4^+$, and 6^+ sequence in each nucleus, and the observed excitation energies are very closely the same in each.^{1,19} However, a striking departure from the $(f_{7/2})$ prediction is observed in the case of Ca^{42} , in that additional levels at 1.836 MeV (0^+) and 2.423 MeV (2^+) have been found. These additional levels do not fit easily into a simple shell-model coupling scheme. One can obtain additional 0^+ and 2^+ levels by including $p_{3/2}$ admixtures in the shell-model calculations.²¹ In order to obtain a 0^+ state at such a low excitation energy, it has been found necessary to couple the shell-model states to deformed states.^{21,23} A measurement of transition rates between the low-lying levels should provide a sensitive test of any theory advanced to explain such levels. In particular, the calculations which employ deformed states predict considerable collective enhancements of these transition rates. The

* Work supported in part through funds provided by the U.S. Atomic Energy Commission under Contract No. At(30-1)-2098.

† Present address: Eastern Washington State College, Cheney, Wash.

¹ C. M. Braams, thesis, Utrecht, 1956 (unpublished); and Phys. Rev. **101**, 1764 (1956).

² P. M. Endt and C. M. Braams, Rev. Mod. Phys. **20**, 683 (1957).

³ W. Buechner and Mazari, Rev. Mex. Fis. **7**, 117 (1958).

⁴ P. M. Endt and C. van der Leun, Nucl. Phys. **34**, 1 (1962).

⁵ P. C. Rodgers and G. E. Gordon, Phys. Rev. **129**, 2653 (1963).

⁶ R. Middleton and D. J. Pullen, Nucl. Phys. **51**, 77 (1964).

⁷ N. Benczer-Koller, M. Nessim, and T. H. Kruse, Phys. Rev. **123**, 262 (1961).

⁸ S. M. Matin, D. J. Church, and G. E. Mitchell, Phys. Rev. **150**, 906 (1966).

⁹ H. Morinaga, N. Mutsura, and M. Sugarawa, Phys. Rev. **114**, 1146 (1959).

¹⁰ J. D. McCullen and J. J. Kraushaar, Phys. Rev. **122**, 555 (1961).

¹¹ E. P. Lippincott and A. M. Bernstein, Phys. Rev. **163**, 1170 (1967).

¹² J. H. Bjerregaard, O. Hansen, O. Nathan, R. Chapman, S. Hinds, and R. Middleton, Nucl. Phys. **A103**, 33 (1967).

¹³ R. J. Peterson, thesis, University of Washington 1966 (unpublished).

¹⁴ D. C. Williams, J. D. Knight, and W. T. Leland, Phys. Rev. **164**, 1419 (1967).

¹⁵ E. P. Lippincott, thesis, Massachusetts Institute of Technology (unpublished).

¹⁶ P. C. Simms, N. Benczer-Koller, and C. S. Wu, Phys. Rev. **121**, 1169 (1961).

¹⁷ F. R. Metzger and G. K. Tandon, Phys. Rev. **148**, 1133 (1966).

¹⁸ H. L. Scott, R. N. Horoshko, and F. R. Rauch, Bull. Am. Phys. Soc. **13**, 696 (1968).

¹⁹ H. Morinaga and E. Bleuler, Phys. Rev. **100**, A1236 (1955).

²⁰ J. D. McCullen, B. Bayman, and L. Zamick, Phys. Rev. **134**, B515 (1964).

²¹ B. J. Raz and M. Soga, Phys. Rev. Letters **15**, 924 (1965).

²² B. H. Flowers and L. D. Skouras (private communication).

²³ W. J. Gerace and A. M. Green, Nucl. Phys. **93**, 110 (1967).

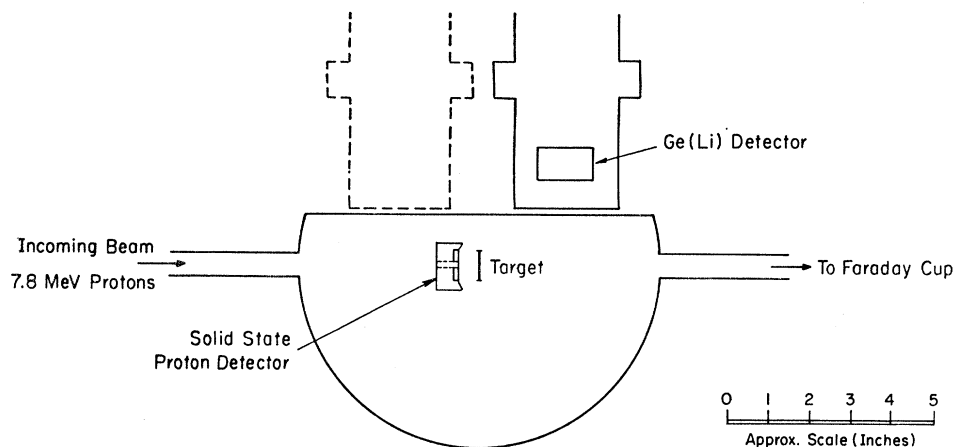


FIG. 1. Schematic of experimental arrangement.

present study was undertaken to provide a test of the theories advanced to explain the "spurious" positive-parity states by studying branching ratios and lifetimes.

II. EXPERIMENTAL METHOD

The bulk of the data reported in this study was obtained with the detector arrangement shown in Fig. 1, consisting of a 500- μ annular silicon-surface barrier detector for the back-scattered protons, and a Ge(Li) detector for the γ rays.

A. Nuclear Excitation

Target nuclei were excited by 1.5 nA of 7.8-MeV protons from the M.I.T. cyclotron. A magnetic quadrupole pair focused these particles to a spot 2 mm in diam. The incident-beam energy spread is approximately 25 keV. The target (of areal density 1.19 mg/cm²) was enriched with Ca⁴² obtained from Oak Ridge National Laboratory of the following compositions¹¹: 4.96% Ca⁴⁰, 93.7% Ca⁴², 0.19% Ca⁴³, 1.18% Ca⁴⁴, <0.02% Ca⁴⁶, and <0.02% Ca⁴⁸. There was also some carbon and oxygen contamination, but this did not prove troublesome. The unscattered protons lose approximately 40 keV in passing through the target, while typical protons inelastically scattered from the downstream side of the target lose 60 keV in passing back through the target. The back-scattered protons were detected in a 500- μ annular silicon detector which had 40-keV resolution (full width at half maximum). The active surface was 15 mm from the target with an inner radius of 2.5 mm and an outer radius of 9 mm, so that its solid angle was 0.8 sr. At a beam intensity of 1.5 nA, about 15 000 protons per second were detected. The observed proton spectrum is shown in Fig. 2. The full width at half maximum (FWHM) obtained on the isolated peaks was 120 keV, which is consistent with uniform excitation throughout the target.

In our treatment of the Doppler-shift measurements, we make use of the assumption of uniform excitation throughout the target to calculate the effect on the

Doppler shift of those recoiling ions that leave the target. We did not select the energy of the protons, so that all the associated recoiling ions would be stopped in the target. We could have done this for an isolated state by only looking at the highest-energy protons leading to this state, i.e., protons for which the reaction

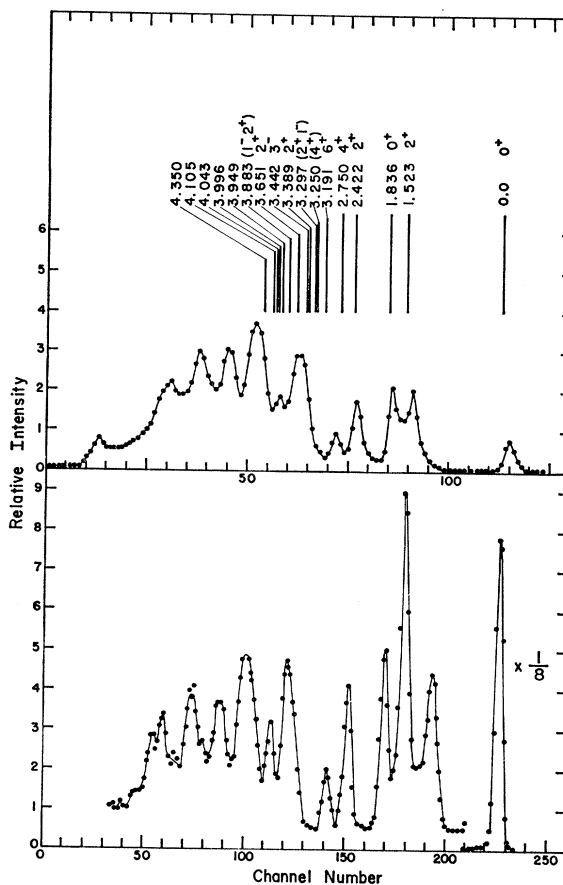


FIG. 2. Proton spectra as observed with the annular detector. The lower spectrum is a single spectrum, while the upper is the spectrum of protons for which a γ ray was coincident.

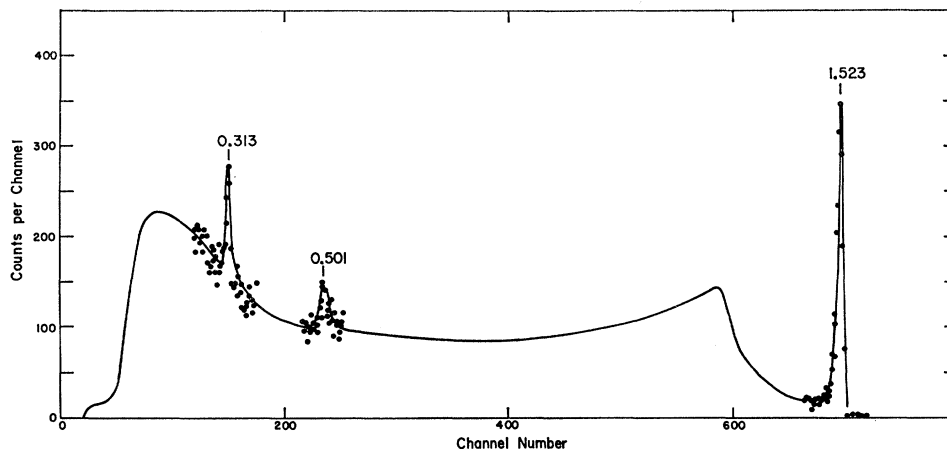


FIG. 3. γ -ray spectrum observed in coincidence with the proton group corresponding to the 1.523-MeV 2^+ states in Ca^{42} .

took place on the entrance side of the target. To further check the assumption of uniform excitation throughout the target, we compared the proton spectrum obtained (with the previously described target at 90° to the beam) to that obtained with the target at 45° to the beam. There were no marked differences in the spectra. This result was unambiguous for the 2_1^+ , 0_2^+ , 2_2^+ , 4_1^+ , and the 2^+ state at 3.651 MeV, since these were isolated. We also obtained a proton spectrum from a thin ($50 \mu\text{g}/\text{cm}^2$) $\text{Ca}^{42}\text{CO}_3$ target. The spectrum so obtained was very similar to the thick target spectrum. The isolated peaks did not vary in relative intensity between thick and thin targets by more than 10%. From the above we can assert that nonuniform excitation, at least for the isolated levels, can only produce errors small in comparison to the statistical error in our nuclear-lifetime measurements. We now make the reasonable assumption that this same conclusion will hold for the nonisolated states which were studied.

B. Gamma Rays

The γ rays were detected with a 32-cc Ge(Li) detector fabricated in this laboratory. This detector was about 12 cm from the target in either of the two positions shown in Fig. 1. These correspond to angles of 55° and 125° measured with respect to the beam. In an early version of this experiment,²⁴ a commercially made 15-cc Ge(Li) detector was used. However, since the 32-cc detector has a photoefficiency approximately five times greater, the earlier data were superseded by the present system.

Since the effective mean position of the Ge(Li) detector was not defined very accurately by the position of the cooling assembly, these angles were checked by Doppler-shift data as described under the section entitled "Doppler-Shift Measurements."²⁴ With the exception noted below, all γ -ray data reported in this experiment were obtained at these two angles. The efficiency

²⁴ W. J. Kossler, T. Ophel, M. Slade, and A. M. Bernstein, *Bull. Am. Phys. Soc.* **12**, 586 (1967).

of the detector as a function of γ -ray energy was measured by employing a number of radioactive sources. A radium source, for which relative intensities of the various lines were obtained from the measurements of Dzhelepov *et al.*,²⁵ proved to be very useful in this regard. Absolute efficiency determinations were made with the aid of Cs^{137} , Co^{60} , and ThC'' sources by comparison against a 3 in. \times 3 in. NaI(Tl) detector. Both procedures yielded the same relative efficiency curve. The double escape-to-photopeak efficiency ratio was also measured up to the 2.614 MeV line of the ThC'' source.

Figures 3, 4, and 5 show typical coincidence γ spectra obtained in this experiment. The energies of the γ rays refer to the transitions indicated in Fig. 13. The coincidence-gating requirements on these spectra are explained below. The resolution obtained with the 32-cc detector was about 8 keV (FWHM) on the 1.523-MeV photopeak in Fig. 4, and was about 5.5 keV (FWHM) on the 1.332-MeV line from Co^{60} .

Corrections for a small zero and gain shift between the data taken at the two angles were made by referring to the 1.836 0^+ -state decay. The lifetime¹⁶ for this state greatly exceeds the stopping time of the recoiling nucleus. The inelastically scattered protons leading to this state were energy selected in such a way that the associated recoil ions stopped in the target.

C. Electronics

Signals from the Ge(Li) detector were amplified by means of a field-effect-transistor preamplifier and a TC-200 shaping amplifier. After differentiation (1.6- μsec time const) a "fast" signal was fed through cascaded fast amplifiers to a fast discriminator of the Brookhaven type.²⁶ The output of the fast discriminator was fed to one input of a time-to-height (TH) con-

²⁵ B. S. Dzhelepov, N. N. Zhukovskii, I. F. Uchevatkin, and S. A. Shestopolova, *Izv. Akad. Nauk. SSSR. Ser. Fiz.* **22**, 835 (1958).

²⁶ R. Sugarman, F. C. Merritt, and W. A. Higginbotham, Brookhaven National Laboratory Report No. BLN 711 (T-248) (1962).

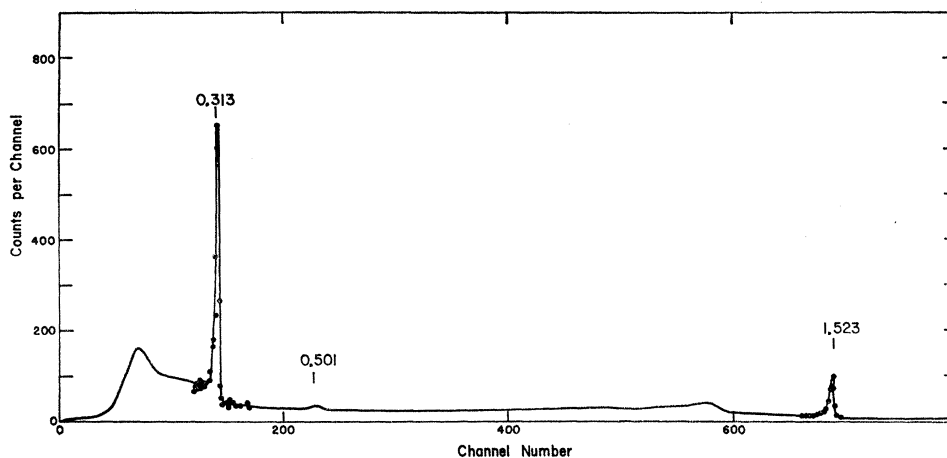


FIG. 4. γ -ray spectrum observed in coincidence with the proton group corresponding to the 1.836-MeV 0^+ state in Ca^{42} .

verter. The output of the TC-200 amplifier after integration (1.6- μ sec time const) was fed to one side of a Nuclear Data 4096 Dual analog-to-digital converter (ADC).

Signals from the proton detector, after preamplification, were sent to both a fast amplifier and a shaping amplifier. The output of the latter amplifier fed the other side of the 4096 ADC. The "fast" signal was used to trigger a fast discriminator, the output of which fed the second input of the TH converter. This TH converter was of the "overlap" type; that is, the size of its output signal is proportional to the time overlap of the two input signals. This feature proved to be very convenient for analyzing the time resolution of various elements of the "fast" circuitry. Some evidence for a time-to-energy correlation was found in the Ge(Li) signal. However, by an appropriate setting of a lower-level discriminator of the TH-converter output, it was possible to obtain an over-all time resolution of $2\tau = 60$ nsec, with essentially 100% acceptance of all γ pulses of $E \gtrsim 100$ keV. We arranged the timing of the γ -ray

discriminator with respect to that of the protons, so that this 2τ corresponds to timing variations of ± 30 nsec. This performance was quite satisfactory, since the cyclotron beam bursts are 3 nsec in duration, with a separation of 74 nsec.

Energy information for both proton and γ -ray events was stored on magnetic tape in the form of an 18-bit word for each coincidence event (7 bits for the proton signal and 11 bits for the γ -ray signal). Since the dual ADC's were operated in a coincidence mode, energy data were recorded only if a proton- γ -ray coincidence occurred. This method of data storage proved to be very convenient for later analysis by means of a system of "read" electronics, since by an appropriate setting of digital gates the γ -ray spectrum in coincidence with any selected portion of the proton spectrum could easily be obtained (or vice-versa). For example, the data of Fig. 3 were obtained by analyzing the magnetic-tape data for the spectrum of γ rays in coincidence with the protons inelastically scattered from the 1.523-MeV state of Ca^{42} .

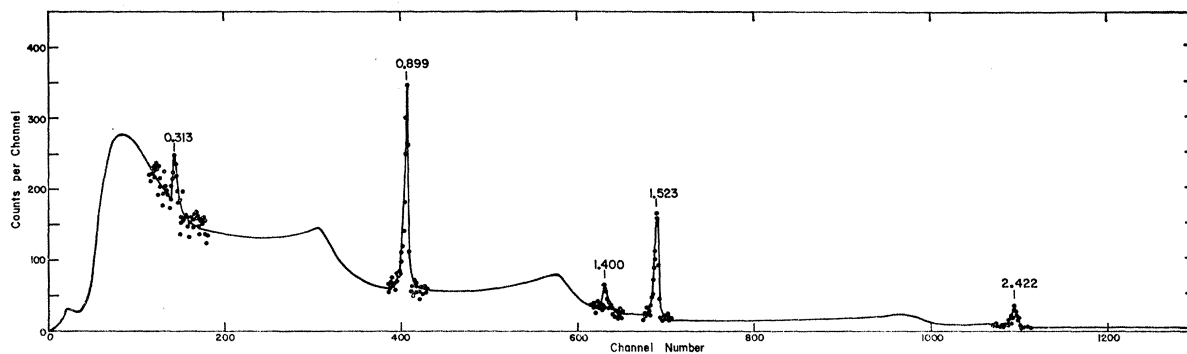


FIG. 5. γ -ray spectrum observed in coincidence with the proton group corresponding to the 2.422-MeV 2^+ state in Ca^{42} .

An additional feature of this method of data storage is that the events are stored in time sequence, making it possible to check for zero or gain shifts.

D. Elimination of Kinematic Broadening

It may be of interest to note that both the proton detectors used in this experiment were of the position-sensitive type. It was thus possible, by a suitable pulse-addition network, to largely eliminate effects of kinematic broadening on the proton resolution. This turned out to be an important consideration for the rectangular detector, where a 25% improvement in resolution was achieved. In the case of the annular detector, no noticeable effect was obtained. This is not surprising since the angular range is less, the energy variation with angles is small at back angles, and most of the energy spread is caused by the variation in energy loss in the target.

III. DATA ANALYSIS

A. Branching Ratios

Branching ratios for the Ca^{42} levels excited in this experiment were obtained from coincidence γ -ray data like that of Figs. 4, 5, and 6. In all cases, the γ peaks were well isolated and peak areas could be easily computed with an allowance made for a linear background. In many cases, the background subtraction constituted the principal source of error quoted for the branching ratios. Data for the two γ -detection angles were averaged with appropriate statistical weights. When double escape peaks could be observed, these were also included in the branching computation.

It might at first appear that the procedure for deriving branching information from observations at only two angles assumes isotropy of the γ -ray angular distribu-

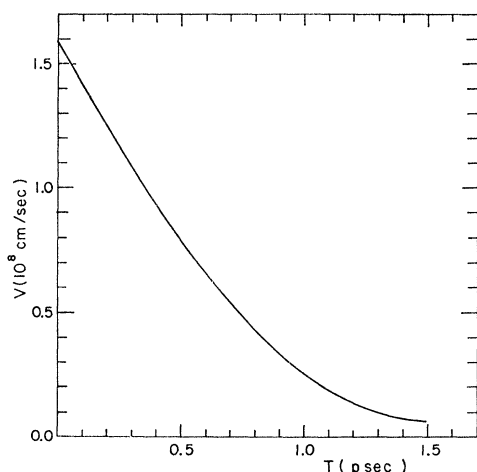


FIG. 6. The mean velocity ($v \cos \varphi$) as a function of time for a Ca^{42} ion excited to the 1.523-MeV 2^+ state by 7.8-MeV protons inelastically scattered into the annular detector.

tions. However, it should be noted that the two angles used (55° and 125°) are zeros of $P_2(\cos\theta)$. Thus, the only source of error in the branching ratios from angular correlation effects would be due to the (presumably) small term $a_4 P_4(\cos 55^\circ)$. The acceptance angular range of the particle detector is fairly large ($172^\circ \rightarrow 149^\circ$), so that the a_4 term should not be much different from that predicted for γ -ray angular distribution. For the angular distribution of a $2^+ \rightarrow 0^+$ γ -ray distribution, a typical value for a_4 is 0.15, as we infer from the review article of Sheldon and Van Patter.²⁷ Since $P_4(\cos 55^\circ) = -0.38$, this implies that we make a 6% error when we compare this transition to a $2^+ \rightarrow 2^+$, predominantly $M1$, transition for which $a_4 = 0$. From these considerations, we put the uncertainty for branching ratios, subject to this kind of uncertainty at 10%. In Table I, only the statistical errors are indicated.

For the 2.422-MeV 2^+ state, a check was made to see whether an $a_4 P_4(\cos 55^\circ)$ contribution might be unexpectedly large in the branching ratios. A rectangular solid-state proton detector was used in place of the annular detector of Fig. 2. This detector was placed at 90° to the incident beam, and subtended approximately 40° in the scattering plane. The purpose of this arrangement was to average over a wide range of scattering angles and thus to partially smear out any angular correlation effects. In this version of the experiment, a 3 in. \times 3 in. NaI(Tl) γ -ray detector was placed 5.72 cm from the target and diametrically opposite to the proton detector. In this case the NaI spectrum was analyzed with the Fortran IV code FITTER,²⁸ which is capable of resolving γ -ray spectra contained in up to 512 channels, into as many as 10 components, by means of a least-squares procedure. The branching ratios measured with this system give the same values as those obtained from the Ge(Li) data taken with the annular proton detector. The Ge(Li) detector and geometry were used for all the rest of the branching information presented in Table I.

B. Doppler-Shift Measurements

The nuclear lifetimes reported here were measured by the Doppler-shift attenuation method (DSAM), which has been used previously and described in some detail by other workers.²⁹⁻³¹ The Doppler shift for a γ ray of unshifted energy E_γ , emitted in a direction given by the unit vector \mathbf{D} by a nucleus of velocity \mathbf{V} , is given to first order in V/c by

$$\delta E = (E_\gamma/c) \mathbf{V} \cdot \mathbf{D}. \quad (1)$$

²⁷ E. Sheldon and D. M. Van Patter, Rev. Mod. Phys. **38**, 143 (1966).

²⁸ T. Ophel (private communication).

²⁹ J. R. MacDonald, D. F. H. Start, R. Anderson, A. G. Robertson, and M. A. Grace, Nucl. Phys. **A108**, 6 (1968).

³⁰ E. K. Warburton, J. W. Olness, and A. R. Poletti Phys. Rev. **160**, 938 (1967).

³¹ A. R. Poletti, E. K. Warburton, J. W. Olness, and S. Hecht, Phys. Rev. **162**, 1040 (1967).

The observed Doppler shift is the difference in peak positions between the spectra taken at 55° and 125° with respect to the beam. For a given nuclear velocity and point detector at positions symmetric around 90° from the velocity of the nucleus, such as the 55° and 125° pair, this observed Doppler shift is twice the shift given by Eq. (1), where now D refers to the smaller-angle detector position. In order to compute the actual Doppler shifts one must consider the following effects:

(a) The magnitude of the velocity is time-dependent and its direction wanders.

(b) The initial directions of the recoiling nuclei fall into a cone because the detected protons are detected in a finite annular detector (near 180° with respect to the beam).

(c) The γ -ray detector has a finite size and its position is not accurately measured.

We take these up one at a time:

(a) At any given time, after the inelastic proton scattering, the average velocity of the recoiling ions will be in the same direction as the initial impulse. This average velocity is the average over trajectories of $V(t) \cos\phi_s(t)$, where $V(t)$ is the speed of the ion, and $\phi_s(t)$ is the angle which the trajectory makes with the initial direction. Lindhard, Scharff, and Schiott³² (LSS) describe calculations for the average speed, which we call $\langle V(t) \rangle$. Blaugrund³³ has pointed out that the straggling angle is often important and describes methods for calculating the average angle $\phi_s(t)$. To obtain the average velocity we make the usual approximation,³³ namely, that the correlation, at a given time, between the speed and straggling angle is not important, and that this average velocity is the product of the averages $\langle V(t) \rangle$ and $\langle \cos\phi_s(t) \rangle$. We calculated this quantity according to the formulas of Blaugrund and LSS. In the calculations, the dimensionless energy loss $d\epsilon/d\rho$, defined by LSS, was approximated by

$$d\epsilon/d\rho = k_0\epsilon^{1/2} + k_n\epsilon^{-1/2}. \quad (2)$$

In this equation k_0 is the electronic stopping constant, which we set equal to 1.2×0.151 ; i.e., we have increased the theoretical value by 20% as we inferred from Northcliffe³⁴ and Ormrod *et al.*³⁵ The parameters k_n , associated with atomic stopping, we set equal to 0.4.^{32,33} Below $\epsilon = 1.2$, the form of the atomic-stopping contribution was inserted explicitly from the calculations of LSS. The mean velocity as a function of time, for Ca^{42} ions excited to the 1.523-MeV state by 7.8-MeV protons inelastically scattered into the annular detector, is shown in Fig. 6. The initial speed is given by the kinematics of the reaction.

³² J. Lindhard, M. Scharff, and H. E. Schiott, Kgl. Danske Videnskab. Selskab. Mat.-Fys. Medd. **33**, 14 (1963).

³³ A. E. Blaugrund, Nucl. Phys. **88**, 501 (1966).

³⁴ L. C. Northcliffe, Ann. Rev. Nucl. Sci. **13**, 67 (1963).

³⁵ J. H. Ormrod, J. R. MacDonald, and H. E. Duckworth, Can. J. Phys. **43**, 275 (1965).

(b) The minimum and maximum scattering angles of the protons (149° and 172°) were used to calculate the minimum and maximum angles for the initial recoil direction of the ions. The solid-angle weighted average was then used to find a mean recoil angle θ_r . The cosine of this cone angle was used as a factor in the calculation of the short lifetime limit for the observable Doppler shift ΔE_0 .

(c) For a γ -ray detector angle θ_d , an angle near to neither 0° nor 180° (an angle such as the present 55°), the small finite size of the detector broadens, but does not shift the photopeak. The average detector angle was checked by observing the Doppler shift for the 4.43-MeV γ ray from C^{12} excited by proton scattering. The observed shift is shown in Fig. 7. Since the known lifetime is short [$(5.9 \pm 0.2) \times 10^{-11}$ sec],^{36,37} the attenuated Doppler shift is 90% of the short lifetime limit. The calculation of this attenuated Doppler shift was carried out in the manner described below. By this technique we obtained $\theta_d = 55^\circ \pm 2^\circ$, in agreement with our geometrical measurement.

Keeping in mind the foregoing considerations, the mean observable Doppler shift may be written as

$$\Delta E = \left[\frac{2E}{c} \gamma \cos(\theta_r) \cos(\theta_d) \right] \times \int_0^\infty V(T) \cos\phi_s(t) \frac{\exp(-t/\tau_m)}{\tau_m} dt, \quad (3)$$

where the factor in square brackets is the short lifetime limit ΔE_0 for the measurable Doppler shift. We in fact

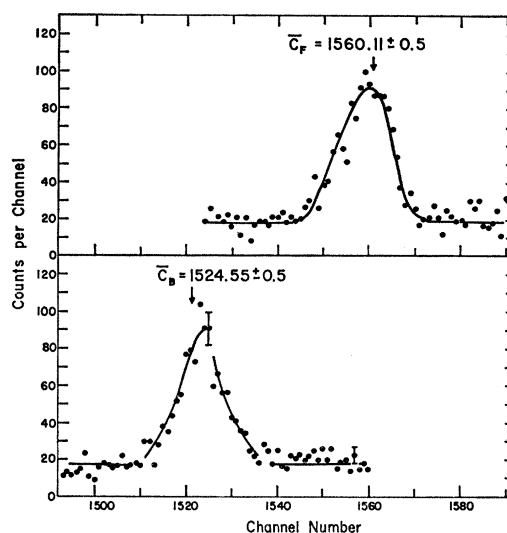


Fig. 7. The observed γ -ray Doppler shift for the 4.43-MeV 2^+ state of C^{12} excited by 7.8-MeV protons inelastically scattered into the annular detector for the usual (55° and 125°) γ -ray detector positions.

³⁶ H. L. Crannel and T. A. Griffy, Phys. Rev. **136**, B1580 (1964).

³⁷ V. K. Rasmussen, F. R. Metzger, and C. P. Swann, Phys. Rev. **110**, 154 (1958).

TABLE I. Branching ratios.

Initial state		E (MeV)	Final state		Transition E (MeV)	Branching ratio γ rays
J ^π	J ^π		J ^π	E (MeV)		
2 ⁺		1.523	0 ⁺	0.0	1.523	1.0
0 ⁺		1.836	2 ⁺	1.523	0.313	1.0
2 ⁺		2.422	0 ⁺	0.0	2.422	0.307±0.013
			2 ⁺	1.523	0.899	0.693±0.013
			0 ⁺	1.836	0.586	≤0.01
4 ⁺		2.750	2 ⁺	1.523	1.227	0.990±0.0037
			2 ⁺	2.422	0.328	0.010±0.0037
6 ⁺		3.191	4 ⁺	2.750	0.44	1.0
(4 ⁺)		3.250	4 ⁺	2.750	0.500	0.37±0.038
			2 ⁺	1.523	1.727	0.576±0.041
			2 ⁺	2.422	0.828	0.051±0.036
(2 ⁺ 1 ⁻)		3.297	2 ⁺	2.422	0.875	0.854±0.048
			2 ⁺	1.523	1.774	0.099±0.031
			0 ⁺	0.0	3.297	0.0259±0.038
			0 ⁺	1.836	1.461	0.0217±0.038
2 ⁺		3.389	0 ⁺	0.0	3.389	0.433±0.027
			2 ⁺	1.523	1.866	0.483±0.021
			0 ⁺	1.836	1.553	0.059±0.018
			2 ⁺	2.422	0.967	0.026±0.021
3 ⁻		3.442	2 ⁺	1.523	1.919	0.571±0.035
			2 ⁺	2.422	1.020	0.391±0.035
			4 ⁺	2.750	0.692	0.037±0.015
2 ⁺		3.651	0 ⁺	0.0	3.651	0.155±0.026
			0 ⁺	1.836	1.815	0.089±0.039
			2 ⁺	1.523	2.128	0.754±0.040
(1 ⁻ 2 ⁺)		3.883	0 ⁺	0.0	3.883	0.50±0.12
			0 ⁺	1.836	2.047	0.50±0.12
		4.043	2 ⁺	1.523	2.520	0.579±0.081
			4 ⁺	2.750	1.293	0.121±0.092
			3 ⁻	3.442	0.601	0.131±0.035
			2 ⁺	2.422	1.621	0.170±0.058
(0 ⁺)		4.105	2 ⁺	1.523	2.577	0.884±0.081
			2 ⁺	2.422	1.678	0.116±0.081
(4 ⁺)		4.35	2 ⁺	1.523	2.827	0.15±0.14
			4 ⁺	2.750	1.600	0.52±0.27
			6 ⁺	3.191	1.160	0.17±0.33
			4 ⁺	3.250	1.100	0.15±0.15

calculated the quantity

$$S = (1 - \bar{\Delta}E/\Delta E_0) \int_0^\infty \left(1 - \frac{V(t)}{V_0} \cos \phi_s(t)\right) \times \frac{\exp(-t/\tau_m)}{\tau_m} dt, \quad (4)$$

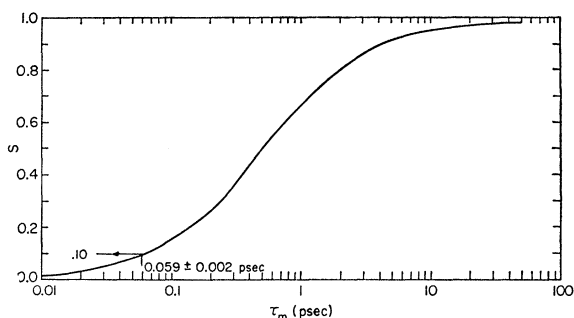


FIG. 8. The function S which is equal to $1 - \Delta E/\Delta E_0$ for the Ca^{42} ion excited to the 4.43-MeV state, stopping in Mylar.

where V_0 is the initial recoil speed of the ion. This quantity S is plotted as a function of mean life in Figs. 8, 9, and 12.

As a check on our techniques we compared our

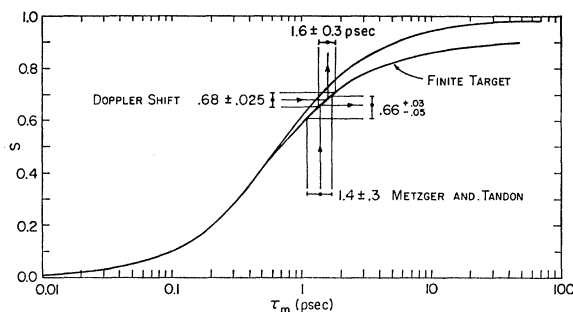


FIG. 9. The function S versus t_m for the 1.523-MeV 2^+ state. The measurement of Metzger and Tandon is by resonance fluorescence and predicts the S to be $0.66(+0.03, -0.05)$. The curve designated as Finite Target includes the correction for recoiling ions leaving the target.

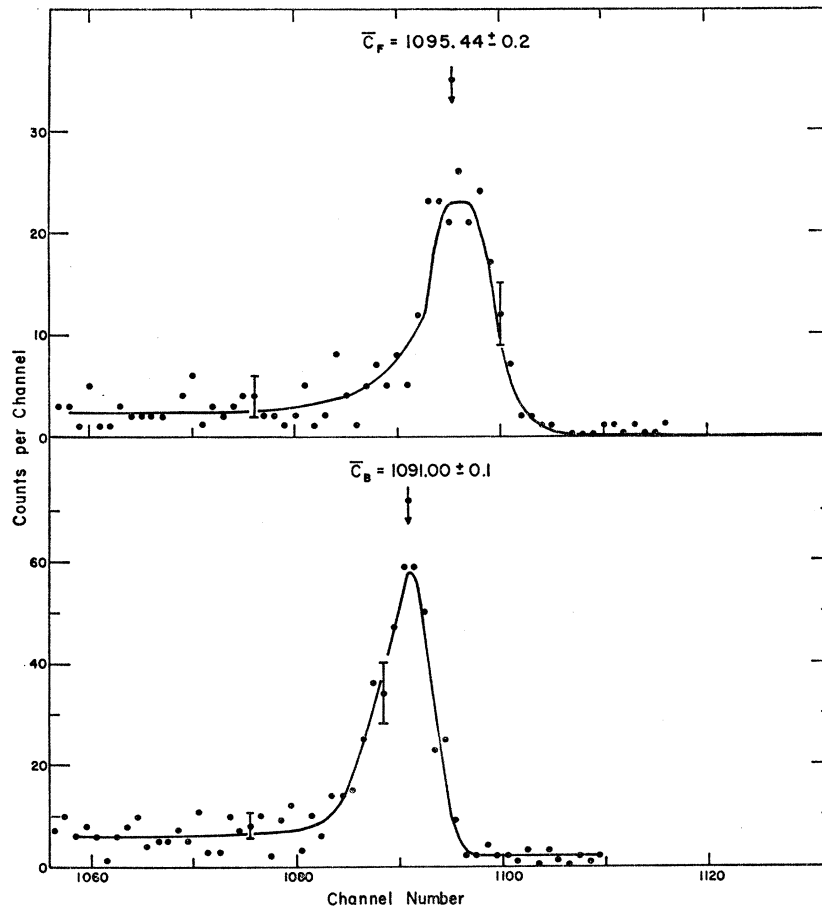


FIG. 10. The observed photopeaks for the $2s^+ \rightarrow 0s^+$ transition. The transition energy is 2.422 MeV. \bar{C}_F is the mean peak position with the γ -ray detector in the forward (55°) position, while \bar{C}_B is the mean peak position with the detector in the backward (125°) position. The channel shift (4.44 ± 0.38) corresponds to an energy shift of 9.85 ± 0.84 keV. The short lifetime limit for the measurable Doppler shift for this transition is 14.22 keV.

measured lifetime for the first excited state of Ca^{42} against that measured by Metzger and Tandon.¹⁷ This comparison is shown in Fig. 10. The close agreement gives us confidence in our procedure.

From the γ -ray spectra associated with proton groups we calculated the mean peak positions by using the formula

$$\bar{p} = \frac{\sum_i C_i(\eta_i - b)}{\sum_i \eta_i - b} = \bar{\eta} \frac{P}{N} - \bar{b} \frac{B}{N}, \quad (5)$$

where C_i is the channel number, η_i is the total number counts in the channel, b is the background in a channel (assumed to be the same in every channel), N is the total counts in the region of interest, P is the number of counts in the peak, B is the number of counts in the background, and $\bar{\eta}$, \bar{p} , and \bar{b} are the respective mean values. To calculate the error in \bar{p} we need to know the standard deviations of $\bar{\eta}$ and \bar{b} and then to combine them appropriately for the case of a linear combination of mean values.³⁸ The mean square σ_B^2 for \bar{b} , is $\sum (C_i - \bar{b})^2 b(1/B)$, and if the region contains R channels of flat background this is approximately $\frac{1}{2} R^2$, which is the same expression as that for the moment of

inertia of a stick about its center. To find the standard deviation σ_n^2 for \bar{n} , we note that we can write Eq. (5) as

$$\bar{\eta} = \bar{p}(N/P) + (\bar{b}B/P). \quad (6)$$

This is again a linear combination of mean values. We calculated the standard deviation for the peak σ_p by dividing the full width at half maximum by 2.355. Upon obtaining σ_n^2 , we insert this to find σ_p .

$$\sigma_p = [p^{-1}(\sigma_p^2 + (2B/P)\sigma_B^2)]^{1/2}, \quad (7)$$

which we use for the error in \bar{p} .

Since the error in stopping time is unknown it has *not* been included in the errors for our measurements. We believe that it should not be larger than the statistical error in most cases.

Finally, because our target was not infinitely thick we corrected for those recoiling ions that leave the target (about 18% of the recoiling nuclei). This correction applied to S is shown in Figs. 11 and 12. The correction is small for short lifetimes because the nucleus decays long before it stops.

IV. RESULTS

The branching ratios measured in this experiment are summarized in Table I. Except where noted, the errors

³⁸ S. S. Wilks, *Elementary Statistical Analysis* (Princeton University Press, Princeton, N. J. 1961), p. 188.

indicated are the statistical errors of one standard deviation (σ). The spins and parities will be discussed below. (See Fig. 13.) Energy assignments for states up to and including the 4.043-MeV states are from Endt and Braams² with the exception of the 3.191-MeV state, whose energy we obtained from Buechner and Mazara.³ The energies for the states at 4.10 and 4.35 MeV

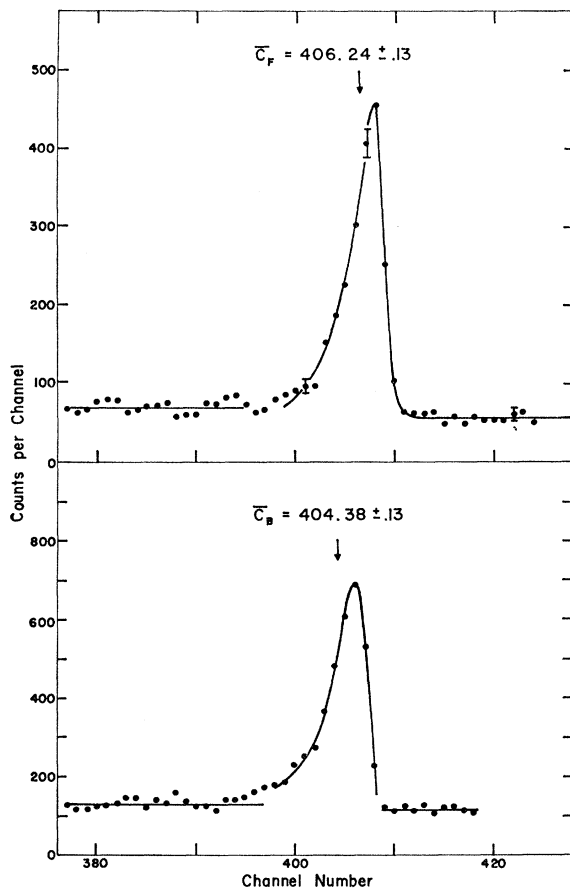


FIG. 11 The observed photopeaks for the $2_2^+ \rightarrow 2_1^+$ transition. The transition energy is 0.899 MeV. \bar{C}_F is the mean peak position with the γ -ray detector in the forward (55°) position, while \bar{C}_B is the mean peak position with the detector in the backward (125°) position. The channel shift (1.86 ± 0.18) corresponds to an energy shift of 4.15 ± 0.35 keV. The short lifetime limit for the measurable Doppler shift for this transition is 5.28 keV.

we obtained from Lippincott and Bernstein.¹¹ With the exception of upper limits, the branching ratios add to unity.

In Table II we have collected the Doppler-shift lifetime information together with lifetimes of the two previously measured states. ΔE_0 is the Doppler shift that would be observed for zero lifetime. S is $1 - \Delta \bar{E} / \Delta E_0$, as was mentioned earlier. τ_m is the *mean* lifetime. The error in the shift comes from the standard deviation of the mean peak position, front and back. One can see from Figs. 10 and 11 how the errors on lifetimes were assigned. No errors for the stopping calculations

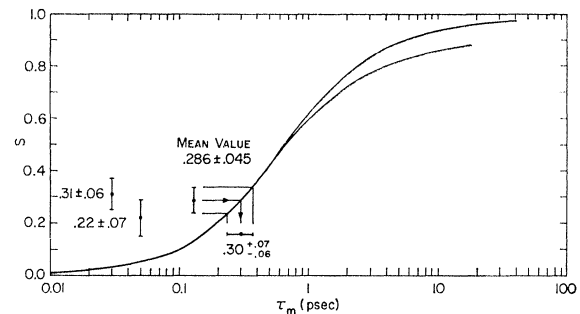


FIG. 12. The function s versus τ_m for the 2.422-MeV 2^+ state. The larger value of s is for the $2_2^+ \rightarrow 2_1^+$ transition. The lower curve at larger τ_m includes the correction for recoiling ions leaving the target.

have been included; i.e., the errors here are the statistical errors only.

The branching ratios and lifetimes were combined to make Table III. The sum of the inverse of the partial lifetimes is the inverse of the lifetime of a state. It may be useful to compare the $B(\sigma\lambda)$ here with the single-particle values of Table IV and the $(f_{7/2})^2$ values shown in Table V.

A. Spins and Parities

The spins and parities of those states up to the 4^+ at 2.750 MeV are well known.^{4,5,8-10}

The 3.191-MeV level is assigned as 6^+ from the $\log(fr)$ and the decay characteristics.⁵ (We observe the same decay for this state.) This state is observed in (t, p) data of Bjerregaard *et al.*,¹² to which we refer below as the (t, p) data and in (α, α') data¹¹ which we call the (α, α') data. The (α, α') angular distribution agrees with this 6^+ assignment.

We observe that the 3.250-MeV state decays to the 4^+ at 2.750 and to the lower two 2^+ states. This restricts the spin values to 2, 3, and 4. From our lifetime measurement we see that if the state were 2^+ , the $E2$ rate to the

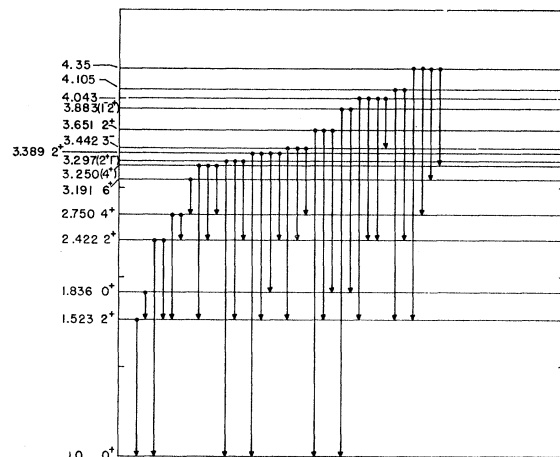


FIG. 13. The observed decays of Ca^{42} . The assignment or inference of spins and parities is described in the text.

TABLE II. Doppler shifts and lifetimes.

J^π	State E (MeV)	E_λ (MeV)	ΔE_0 (keV)	ΔE (keV)	S	Mean lifetime τ_m (psec)
2 ⁺	1.523					1.4±0.3 ^a
2 ⁺	1.523	1.523	9.28	2.93±0.24	0.68±0.025	1.6±0.3
0 ⁺	1.836					480±30 ^b
		2.422	14.22	9.85±0.84	0.31±0.059	
2 ⁺	2.422	0.899	5.28	4.15±0.35	0.22±0.066	0.3(+0.07, -0.06)
4 ⁺	2.750	1.227	7.09	1.57±0.64	0.78±0.09	3.4(+11, -0.17)
6 ⁺	3.191	0.440	2.49	0.022±0.65	0.99±0.25	>0.7(2σ)
(4 ⁺)	3.250	1.727	9.76	6.84±0.93	0.30±0.10	0.3(+0.15, -0.10)
		0.875	4.93	0.84±0.66	0.83±0.13	
(2 ⁺ 1 ⁻)	3.297	1.774	10.0	3.71±2.79	0.63±0.28	3.5(+∞, -2.1)
		3.389	19.01	14.91±1.26	0.21±0.066	
2 ⁺	3.389	1.866	10.5	6.46±0.94	0.384±0.089	0.325±0.075
		1.919	10.7	6.55±1.22	0.39±0.11	
3 ⁻	3.442	1.020	6.80	1.76±1.42	0.74±0.21	0.65±0.2
		3.651	20.2	18.71±2.34	0.074±0.12	
2 ⁺	3.651	2.128	11.77	11.56±2.02	0.018±0.17	0.06(+0.08, -0.06)

^a Measurements of F. R. Metzger and G. K. Tandon.^b Measurements of P. C. Simms, N. Benczer-Koller, and C. S. Wu.

4⁺ state would be about 3000 single-particle units. We therefore exclude this case. Similarly, 2⁻ and 4⁻ may be excluded. The state is observed both in (α, α') and in (t, p) reactions, which strongly implies natural parity; thus we may rule out 3⁺. We rule out 3⁻, and therefore can assign a J^π of 4⁺ for this state on the basis of the systematics of 3⁻ states, for were this state to be a 3⁻ state it would be the lowest 3⁻ state in the spectrum of Ca⁴². Typically, the lowest 3⁻ state is excited in (α, α') scattering more strongly than any other 3⁻ state, while this state is excited with only $\frac{1}{10}$ the strength of the "lowest" 3⁻ state, which is at 3.442 MeV. The assignment of 4⁺ for this state is important, since this then identifies an excellent candidate for the 4⁺ state which, like the 4₁⁺ state, is predicted to be a mixture of a shell-model configuration and a deformed state.^{22,23}

The decay of the 3.297-MeV state to the 2₁⁺, 0₂⁺, and 0₁⁺ limits the spin to 1 and 2, while the fact that it is

observed in (t, p) scattering implies natural parity, so that we have the possibilities $J^\pi=2^+$ or 1⁻.

The levels at 3.389, 3.442, and 3.651 MeV have been observed in (t, p) and (α, α') reactions. The 3.389-MeV level is inferred to be 2⁺ from the (t, p) data, in agreement with the decay characteristics. In fact, the above lifetime and branching ratios demand 2⁺ or 1⁺. The 3.442-MeV state has been assigned 3⁻ and the 3.651-MeV state has been assigned 2⁺ from both the (t, p) and (α, α') data. Our results are not inconsistent with these assignments. This 3⁻ state, which should decay by E1 to the 2₁⁺, is quite inhibited ($\sim 10^8$). This inhibition is apparently a reflection of the character of the 3⁻ state (an octupole vibration). Since the radiation operator is a one-body operator, this state, which is presumably a coherent linear combination of many ($3p, 1h$) states, should have a small E1 matrix element to the simple shell-model ($2p$) and deformed ($4p, 2h$)

TABLE III. Partial lifetimes and $B(\sigma\lambda)$.

Initial state		Final state		Partial lifetime (psec)	$\sigma\lambda$	$B(\sigma\lambda)$ ($e^2f^2\lambda$)
J^π	E (MeV)	J^π	E (MeV)			
2 ⁺	1.523	0 ⁺	0.0	1.4 ^a 1.6±0.2	E2	74±17 62±7
0 ⁺	1.836	2 ⁺	1.523	480±30 ^b	E2	556±34
2 ⁺	2.422	0 ⁺	0.0	0.976(+0.28, -0.22)	E2	10±2.5
		2 ⁺	1.523	0.433(+0.12, -0.08) 11.3(+35.0, ^e -8.0) 0.45(+0.126, -0.1)	E2 M1 E2	123(+300, -80) 0.00192±0.00046 <400
4 ⁺	2.750	2 ⁺	2.422	0.034(+0.11, -0.017)	E2	642(+650, -500)
		2 ⁺	1.523	3.34(+11, -1.7)	E2	85.6(+85, -65)
6 ⁺	3.191	4 ⁺	2.750	>7(2 σ)	E2	<700 ^d
(4 ⁺)	3.250	4 ⁺	2.750	0.81(+0.4, -0.3)	E2 M1	32 000(+20 000, -10 000) ^e 6.21(+4, -2)×10 ^{-3 f}
		2 ⁺	1.523	0.52(+0.25, -0.2)	E2	102(+63, -34)
(2 ⁺)	3.297	2 ⁺	2.422	5.9(+25, -3)	E2	355(+350, -290)
		2 ⁺	2.422	4.09(+∞, -2.47)	E2	389(+500, -389) ^e
2 ⁺	3.389	2 ⁺	1.523	35.3(+∞, -24)	M1	2.3(+1.5, -2.3)×10 ^{-4 f}
		2 ⁺	2.422	0 ⁺	0.0	E2
3 ⁻	3.442	2 ⁺	1.523	135(+∞, -113)	E2	3.18(+2, -3.18)×10 ^{-6 f}
		2 ⁺	2.422	0 ⁺	0.0	E2
2 ⁺	3.651	0 ⁺	0.0	161(+∞, -132)	E2	0.76(+3, -0.76)
		0 ⁺	1.836	0.75±0.18	E2	2.43±0.5
2 ⁺	3.651	2 ⁺	1.523	0.67±0.16	E2	51±13 ^e
		2 ⁺	2.422	5.5±2.1 13±13	M1 E2 E2 M1	(2.5±0.8)×10 ^{-4 f} 16.4±5 74(+∞, -37) ^e [5.3(+∞, -2.7)]×10 ^{-5 f}
2 ⁺	3.651	0 ⁺	0.0	0.39(+0.52, -0.39)	E2	3.2(+∞, -1.9)
		0 ⁺	1.836	0.67(+0.90, -0.67)	E2	61.4(+∞, -35)
2 ⁺	3.651	2 ⁺	1.523	0.80(+1.1, -0.8)	E2	2350(+∞, -1200) ^e
		2 ⁺	2.422	0.080(+0.11, -0.08)	M1	8.2(+∞, -5)×10 ^{-3 f}

^a Measurements of F. R. Metzger and G. K. Tandon.^b Measurements of P. C. Simms, N. Benczer-Koller, and C. S. Wu.^c Using $Z=0.2\pm 0.1$ from S. M. Matin, D. J. Church, and G. E. Mitchell.^d R. A. Mendelson has obtained a lifetime for this state (private communication).^e Assuming 100% E2.^f Assuming 100% M1.

states which make up the 2⁺ states. This explanation is similar to that given in the review article by Perdrisat.³⁹

At 3.883 and 4.043 MeV, there are states which are observed in the (t, p) data. The 3.883-MeV state is also seen in the (α, α') data. Therefore, and since the 3.883-MeV state decays to the 0₁⁺ and 0₂⁺ states, we infer spins 1⁻ or 2⁺. The latter state decays to the 2₁⁺,

4₁⁺, 3₁⁻, and 2₂⁺ states, which then implies spin parities of 2⁺, 3⁻, or 4⁺.

For an excitation near 4.105 MeV, a 0⁺ assignment is made from the (t, p) data. In the (α, α') data, an excitation is seen near this energy which has been assigned 5⁻. We observe a level which decays to the 2₁⁺ and 2₂⁺ states and not to states with higher spin. We therefore support a 0⁺ assignment for a state at 4.105 MeV. That we did not see a state with the decay characteristics corresponding to a 5⁻ state does not rule out the existence of such a state, for in the (p, p') reaction

TABLE IV. Single particle $B(\sigma\lambda)$.

	E1	M1 ^a	E2
$B(\sigma\lambda)$ ($e^2f^2\lambda$) ^b	0.249	0.02639	8.67

^a Weisskopf.^b $B_{sp}(E\lambda, \lambda \rightarrow 0) = (e^2/4\pi) \langle r^\lambda \rangle^2$, $\langle r^\lambda \rangle = [3/(3+\lambda)]R_0^\lambda$, and $R_0=1.2$ (42)^{1/2}.³⁹ C. F. Perdrisat, Rev. Mod. Phys. **38**, 41 (1966).TABLE V. ($f_{7/2}$) values for $B(E2)/B(E2)_{sp}$.

	6 ⁺ →5 ⁺	4 ⁺ →2 ⁺	2 ⁺ →0 ⁺
$B(E2)/B(E2)_{sp}$	0.433	0.949	0.952

TABLE VI. Comparison with Gerace and Green and Flowers and Skouras.

Initial state		Final state		$B(E2)_{\text{expt}}$ e^2f^4	FS ^a	GG ^b
J_n^π	E (MeV)	J_n^π	E (MeV)		$B(E2)_{\text{theor}}$ e^2f^4	
2_1^+	1.523	0_1^+	0.0	74 ± 17^c	55	42
0_2^+	1.836	2_1^+	1.523	556 ± 34^d	542	375
2_2^+	2.422	0_2^+	1.836	<400	151	104
		0_1^+	0.0	10 ± 2.5	2.3	12.3
		2_1^+	1.523	$123(+300, -83)$	103	69.2
4_1^+	2.750	2_1^+	1.523	$85.6(+85, -65)$	102	96.3
		2_2^+	2.422	$642(+650, -500)$	23	48.1
4_2^+	3.250	2_1^+	1.523	$102(+63, -34)$	119	83.7
		2_2^+	2.422	$355(+350, -290)$	179	116.2

^a $f_{7/2} = d_{3/2}$ $g_{AD} = 6.05$ MeV $e^{-n_{\text{eff}}} = 0.75$ e , Flowers and Skouras.

^b $\beta = 0.24$ $e^{-n_{\text{eff}}} = 0.5$ e , Gerace and Green. Last five numbers from (private communication).

^c Measurement of Metzger and Tandon.

^d Measurement of Simms, Benczer-Koller, and C. S. Wu.

at our energy 5^- states are much more weakly excited than 0^+ states.

The excitation at 4.35 MeV decays to the 2_1^+ , 4_1^+ , 6_1^+ , and 4_2^+ . It is observed in the (t, p) data. We therefore assign a j^π of 4^+ .

B. Shell Model and Deformed States

The 1.523-MeV 2^+ state decays to the ground state with about eight single-particle units; the 0^+ 1.836-MeV state has been measured by Simms *et al.*²¹ to have a decay rate of about 12 single-particle units. For the 2.422-MeV 2^+ state, our measurement of the lifetime and branching must be used together with the measurement of Matin, Church, and Mitchell⁸ to obtain the $B(\sigma\gamma)$ values in Table III. The ground-state transition is of single-particle strength, while the $2_2^+ \rightarrow 2_1^+$ $E2$ transition is about 10 single-particle units. Most of the error in this rate comes from the error in the mixing ratio. This ratio may soon be available with smaller errors from the measurements of Scott *et al.*¹⁸ Our results for the 4^+ states are less accurate than those for the previously mentioned 2^+ states because of poorer statistics and the fact that the Doppler shifts for these states were out of the most sensitive region of the S versus τ_m curve (see Figs. 9 and 12).

Gerace and Green²³ and Flowers and Skouras²² have carried out calculations on Ca^{42} in which they mix a rotational band ($4p, 2h$) with simple shell-model ($2p$) configurations. In Table VI we present a comparison of the experimental $E2$ reduced matrix elements with those predicted by Gerace and Green, and Flowers and Skouras. There is some agreement between the theoretical predictions and these experimental results. The ratios of the reduced matrix elements $B(E2) (4_1^+ \rightarrow 2_2^+) /$

$B(E2) (4_1^+ \rightarrow 2_1^+)$ and $B(E2) (4_2^+ \rightarrow 2_2^+) / B(E2) (4_2^+ \rightarrow 2_1^+)$ are predicted by Flowers and Skouras to be 0.23 and 1.5, while we obtained 7.5 ± 3 and 3.48 ± 2.5 , respectively. The errors here are due to the branching ratios only. It is clear that the prediction that the upper 4^+ would have a larger reduced matrix element to the upper 2^+ is borne out by the experiment. Further, one sees from Table VI that the prediction that the upper 4^+ would have larger reduced matrix elements than the lower 4^+ is also verified. However, we see that the $B(E2)$ ratio of the lower 4^+ does not agree. The calculated transition rates required a large (0.5 e) effective charge on the neutrons to obtain agreement with the large transition rates for the 2_2^+ , 0_2^+ , and 2_1^+ states. Since the 4^+ states continue to show the strong enhancement which the theory predicts with this large effective charge, these results tend to support this requirement. Finally, we note that the $B(M1)$ for the transition, which we obtain as 0.00192 ± 0.00046 is estimated by Gerace²¹ to be approximately 0.004. Both theoretical and experimental $M1$ rates are an order of magnitude smaller than single-particle reduced matrix elements.

ACKNOWLEDGMENTS

We would like to especially thank Dr. Trevor Ophel for many helpful discussions, for making available the program FITTER, and for taking part in the early stages of this experiment. We are grateful to Professor A. M. Bernstein for critical discussions and for reading the manuscript. We also would like to thank M. Slade for writing some of the computer programs and helping in taking data, and M. Weissberger for helping in taking data.

²¹ W. J. Gerace, thesis, Princeton University 1967 (unpublished).